



# Biogenic synthesis of AuNPs using *Solanum virginianum* L. and their antibacterial, antioxidant and catalytic applications

Preety Rohilla<sup>1</sup> · Ashmita Chhikara<sup>1</sup> ·  
Pushpa Dahiya<sup>1</sup>

Received: 26 April 2023 / Accepted: 11 October 2023 / Published online: 3 November 2023  
© Association of Microbiologists of India 2023

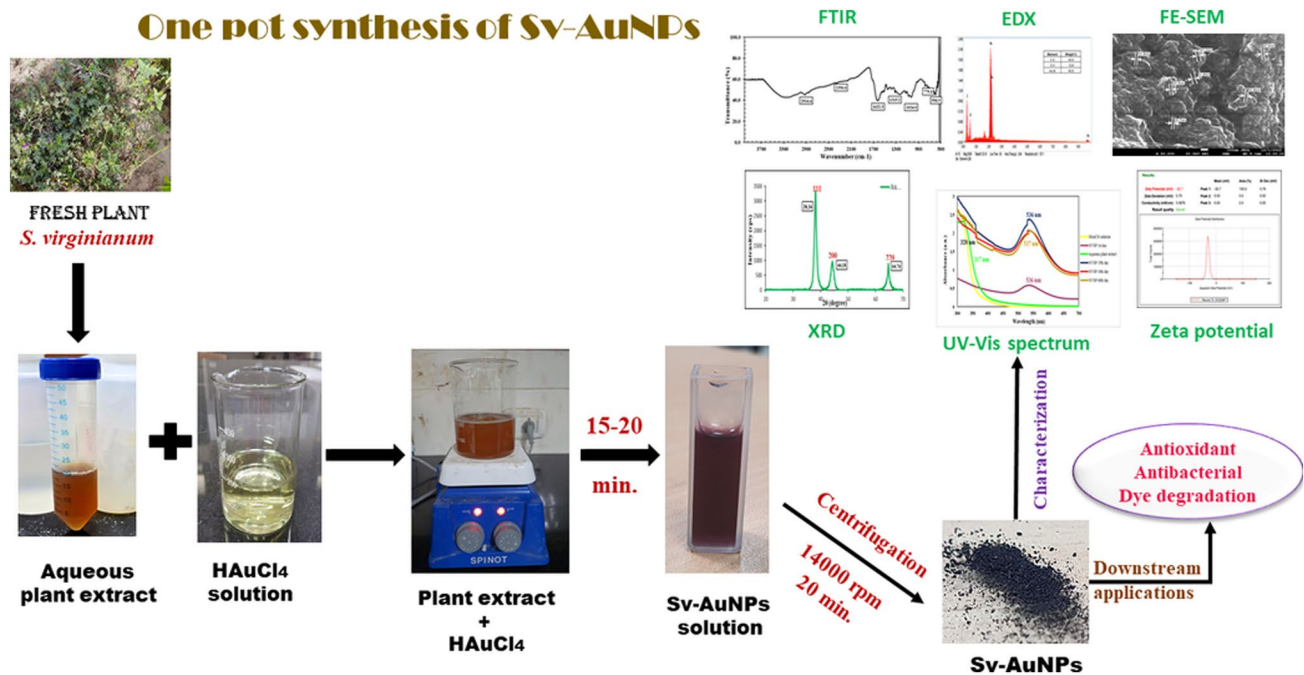
**Abstract** Biogenic synthesis of nanoparticles is gaining popularity worldwide because of being ecofriendly as well as economical, with minimal production of hazardous by-products. The present study was targeted to determine the antibacterial, free radical scavenging and catalytic activity of gold nanoparticles synthesized from *Solanum virginianum* L. (Sv-AuNPs). After addition of auric chloride, the color of aqueous plant extract changed from light yellow to purple-red, indicating the formation of nanoparticles. A strong peak at 536 nm affirmed synthesis of Sv-AuNPs, and negative zeta potential ( $-30.7$ ) indicated their being wrapped in anions. They exhibited face-centered cubic and crystalline nature as revealed by X-ray diffraction. Elemental composition of Sv-AuNPs was ascertained by energy-dispersive X-ray spectroscopy, and a sharp peak at 2.2 keV confirmed the presence

of gold. The shape of Sv-AuNPs synthesized was spherical with size ranging from  $29.1 \pm 1$  nm to  $51.2 \pm 0.7$  nm. Antibacterial potential was evaluated against *E. coli*, *C. violaceum*, *K. pneumoniae*, *P. aeruginosa*, *B. subtilis*, *M. smegmatis*, and *S. aureus* and was found to be greater than aqueous plant extract. Sv-AuNPs exhibited antioxidant potential comparable to ascorbic acid, demonstrating their vital role in the prevention of reactive oxygen species related diseases. Apart from their pharmaceutical potential, these nanoparticles also exhibited promising catalytic efficacy. They degraded harmful dyes i.e. 4-nitro phenol (4-NP) and congo red (CR) at a very low concentration of 50  $\mu\text{g/ml}$ . This is the first report on the antibacterial, antioxidant, and catalytic properties of Sv-AuNPs and we hope it will lead the way for nanoparticles multifunctionality.

✉ Pushpa Dahiya  
pushpa.dahiya@hotmail.com

<sup>1</sup> Department of Botany, Maharshi Dayanand University,  
Rohtak, Haryana 124001, India

## Graphical abstract



**Keywords** Antibacterial · Antioxidant · Sv-AuNPs · Dye degradation · Reactive oxygen species · *Solanum virginianum*

**Abbreviations**

µg/ml	Microgram per milliliter
4-NP	4- Nitrophenol
AuNPs	Gold nanoparticles
CR	Congo Red
DPPH	2, 2-Diphenyl-1-picryl-hydrazyl
DW	Distilled water
EDS	Energy dispersive spectroscopy
FE-SEM	Field emission scanning electron microscopy
FTIR	Fourier transform infrared spectroscopy
mg/ml	Milli gram per milli liter
min	Minutes
mm	Milli meter
mM	Milli molar
NaBH <sub>4</sub>	Sodium borohydride
SPR	Surface plasmon resonance
Sv-AuNPs	<i>Solanum virginianum</i> gold nanoparticles
UV-Vis	Ultra violet-visible spectroscopy
XRD	X-ray diffraction
ZOI	Zone of inhibition

Nanotechnology has been an enthralling topic for almost three decades now, and is gaining more prominence these days due to its vast biomedical applications. Nanoparticles surpass their mass counterparts as they possess small size,

large surface area to volume ratio, and diverse morphologies [1, 2]. Although a number of noble metals are used for nanoparticles synthesis [3–6], but AuNPs are more favorable as their synthesis is relatively simple and does not require high temperature and pressure. Moreover, they possess remarkable optical, electrical, and physicochemical characteristics and exhibits high stability [7–10]. Due to inert nature, their use in diagnosis, photodynamic and photothermal therapy, drug delivery, and imaging is becoming more acceptable [11–14]. As traditionally used physical and chemical approaches for synthesis of nanoparticles are expensive and ecologically harmful, the use of biomimetic method are becoming more prevalent [15, 16]. Biological materials used for synthesis of nanoparticles include bacteria, fungi, algae, viruses, plants and biomolecules. Plants however have an edge over these because they act as a good reducing and stabilizing vehicle and phytosynthesis of nanoparticles requires a shorter time span [17, 18]. Portability, simplicity in handling, absence of necessity to maintain cell cultures, and one-step simplicity of the procedure are another beneficial aspects of phytosynthesis [19–21].

*Solanum virginianum* L. (Solanaceae family) commonly known as ‘Kantakari’ is a main component of an ayurvedic formulation ‘Dashmoola’ used for treating inflammation, respiratory and gastric problems. The plant is widely distributed in Malaya, Sri Lanka, China, India, Bangladesh, Australia, Asia and Polynesia region [22, 23]. Modern pharmacological properties of the plant such as anticancer,

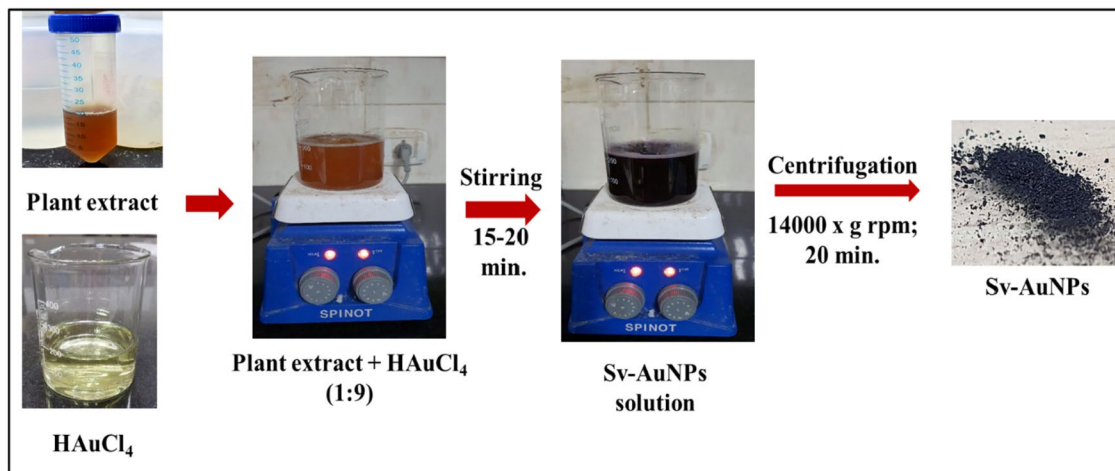


**Fig. 1** Schematic representation of biogenic synthesis of Sv-AuNPs

antipyretic, anti-diabetic, antioxidant, antimicrobial, and anti-inflammatory have claimed its traditional uses [24–27]. Due to its significant contribution to human health, the current study was aimed to fabricate gold nanoparticles from fresh aerial vegetative parts of *S. virginianum* and assess them for their antibacterial and antioxidant potential. Efforts were also made to explore their potential in preventing environment degradation through reduction of harmful dyes. Though Sv-AuNPs have been reported to possess anticancer activity against NCP cell lines [28], this is the very first report regarding their antibacterial, antioxidant, and dye degradation properties.

## Materials and Methods

**Materials** Auric chloride (HAuCl<sub>4</sub>) and DPPH (2, 2-diphenyl-1-picryl-hydrazyl) were obtained from Merck Sigma-Aldrich, India. Ascorbic acid, nutrient agar, nutrient broth, sterile antibiotic discs were supplied by HiMedia. Sodium borohydride (NaBH<sub>4</sub>), Congo red (CR), and 4-nitrophenol (4-NP) were obtained from Qualigens. All the bacterial strains were procured from Microbial Type Culture Collection (MTCC), CSIR-IMTECH, Chandigarh, India.

**Collection of Plant Material and Preparation of Extract** Fresh aerial vegetative parts of *S. virginianum* were collected from Rohtak district, Haryana, India. Plant parts were washed twice with distilled water (DW) to remove impurities and foreign particles. 10 g of plant parts were crushed in 100 ml DW (1:10 w/v) and extraction was carried out in water bath at 60 °C for 30 min. The extract prepared was filtered through Whatman filter paper no. 1 and supernatant obtained was stored in refrigerator till further use.

**Synthesis of Gold Nanoparticles (Sv-AuNPs)** 5 ml of aqueous plant extract was mixed with 45 ml (1:9 v/v) of

freshly prepared auric chloride (1 mM HAuCl<sub>4</sub>) solution [29]. The change in color of the solution after 15–20 min. from light yellow to purple-red confirmed the synthesis of Sv-AuNPs (Fig. 1). Sv-AuNPs were separated from the reaction solution by centrifugation at 14,000 × g rpm for 20 min. After 2–3 washings of the pellet with DW, sample was lyophilized using 120,890-d, Alpha 2–4 LD plus, Martin Christ Freeze Dryer, Germany.

**Instrumental Analysis** UV–Vis spectrum of plant extract, HAuCl<sub>4</sub> and biosynthesized Sv-AuNPs was recorded using Shimadzu UV-3600 Plus, spectrophotometer. UV–Vis spectra of Sv-AUNPs was recorded at different time intervals upto six months to check their stability. Zeta potential and hydrodynamic size distribution report of Sv-AuNPs were estimated using Zetasizer Nano ZS Malvern (version 2.3) at Aryabhata Central Instrumentation Laboratory, MDU, Rohtak. FTIR spectrum of plant extract, HAuCl<sub>4</sub> and Sv-AuNPs was recorded using Thermo Scientific™ Nicolet™ iS50 FTIR Spectrometer over the wavelength range of 500–4000 cm<sup>-1</sup> at the resolution of 4 cm<sup>-1</sup> using KBr pellet method to identify the functional groups. XRD was carried out with a Cu-Kα (k = 1.54 Å) at 40 kV voltage and 20 mA electric current and the spectrum was recorded between 2θ values from 10–70 degrees using MAXima\_X XRD-7000 Shimadzu, Tokyo, Japan. FE-SEM images were captured at different magnifications to check the morphology and size of Sv-AuNPs. The powdered sample was secured with double-sided carbon tape, coated with a thin layer of gold and monograph was recorded using FE-SEM (JSM-7610F Plus/JEOL Schottky Field Emission Scanning Electron Microscope). Elemental composition was analyzed using EDS Bruker X-flash detector (Bruker, Germany). FE-SEM and EDS was performed in Dr. APJ Abdul Kalam Central Instrumentation Laboratory at Guru Jambheshwar University of Science and Technology, Hisar.

### Downstream Applications of Sv-AuNPs

**Antibacterial Studies** Antibacterial potential of plant extract and SV-AuNPs was assessed against *Escherichia coli* (MTCC-41), *Chromobacterium violaceum* (MTCC-2656), *Klebsiella pneumoniae* (MTCC-109), *Pseudomonas aeruginosa* (MTCC-2453), *Bacillus subtilis* (MTCC- 2057), *Mycobacterium smegmatis* (MTCC-992), and *Staphylococcus aureus* (MTCC-96) using disc diffusion assay [30]. To prepare the inoculum, bacterial strains were cultured in HiMedia nutrient broth over the night in shaker cum B.O. D incubator at 37°C. Thereafter, bacterial cultures were calibrated to 0.5 McFarland ( $1.5 \times 10^8$  CFU/ml) and used for further experiments. After being inoculated with 100 µl of bacterial inoculum, nutrient agar plates were impregnated with sterile discs having varying concentrations of Sv-AuNPs (5 mg/ml, 2 mg/ml and 1 mg/ml) and aqueous plant extract (100 mg/ml). DMSO and ampicillin (0.1 mg/ml) were used as negative and positive controls, respectively. The assay was performed in triplicate and average diameter of ZOI was recorded.

**Antioxidant Studies** DPPH assay was carried out to determine the antioxidant activity of aqueous plant extract and Sv-AuNPs [31]. 2 ml of 0.3 mM DPPH solution was added to different concentration of plant extract and Sv-AuNPs (20-100 µg/ml). Ascorbic acid was used as standard. After

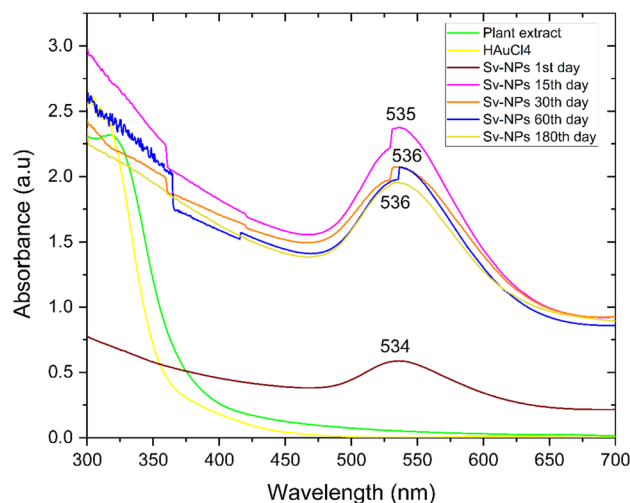


**Fig. 3** UV–Vis spectrum of plant extract, HAuCl<sub>4</sub> and Sv-AuNPs at different time intervals

incubating the sample under dark conditions for 30–35 min, absorbance was recorded at 517 nm. Experiment was performed in triplicate, and mean value was recorded. The following equation was used to calculate the antioxidant activity:

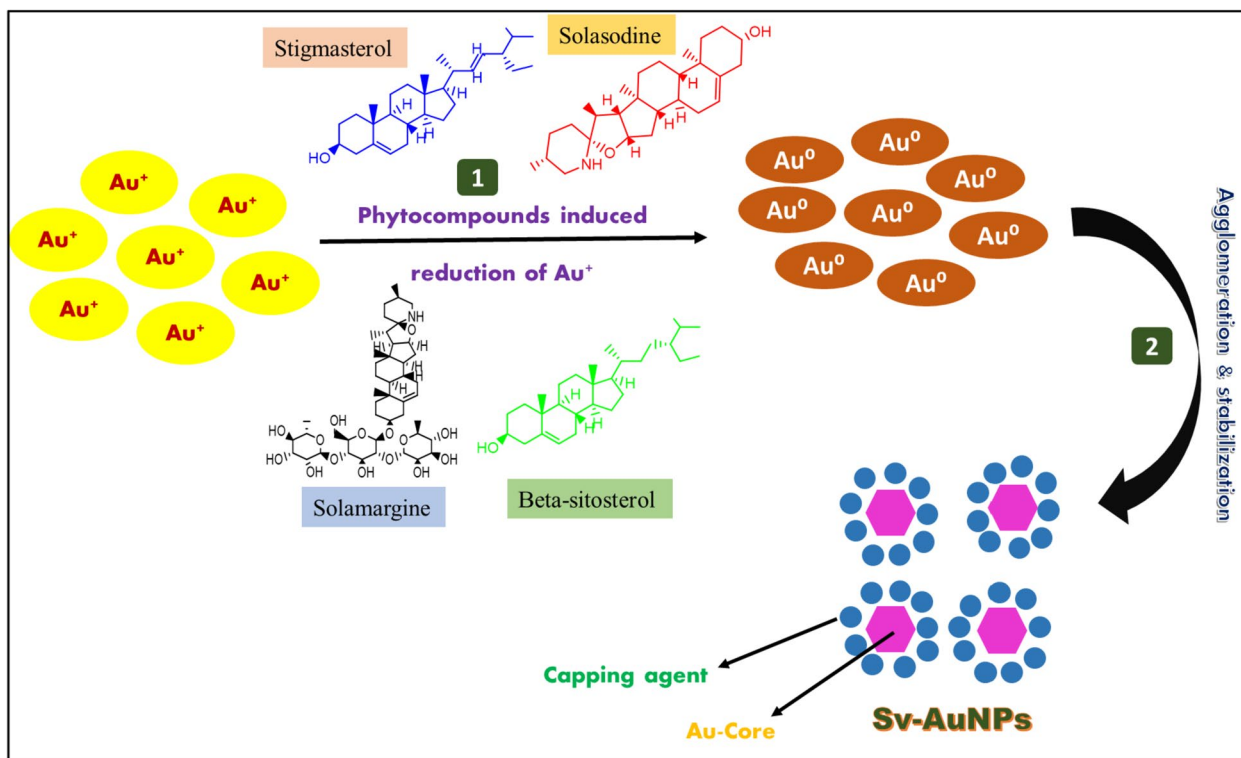


**Fig. 2** Plausible mechanism for biosynthesis of Sv-AuNPs

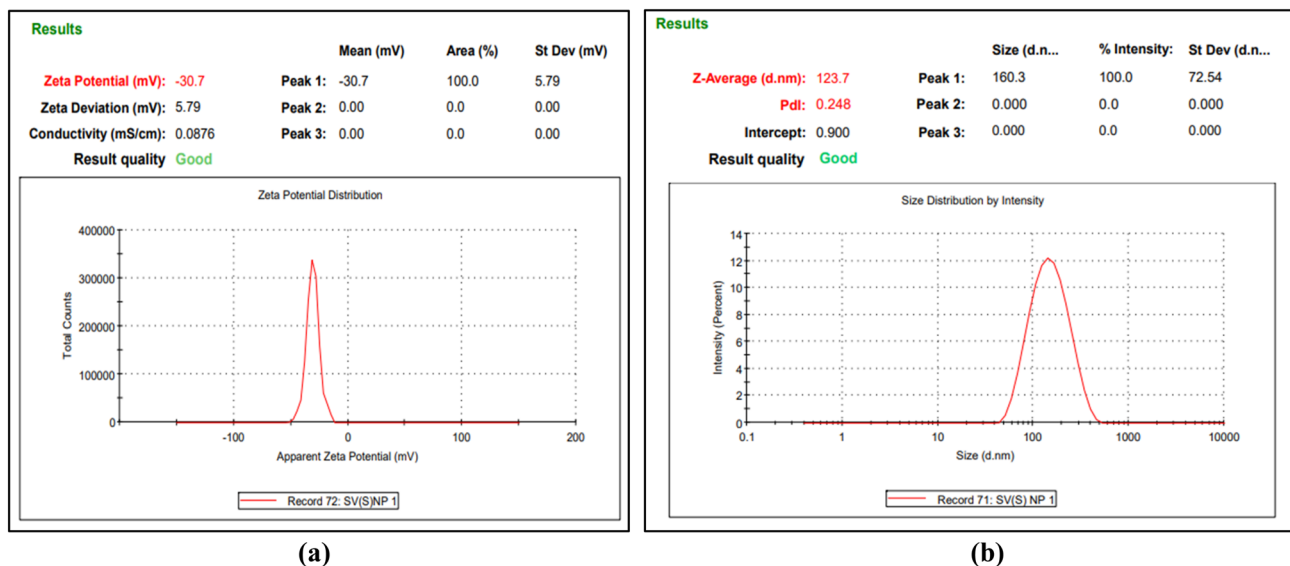
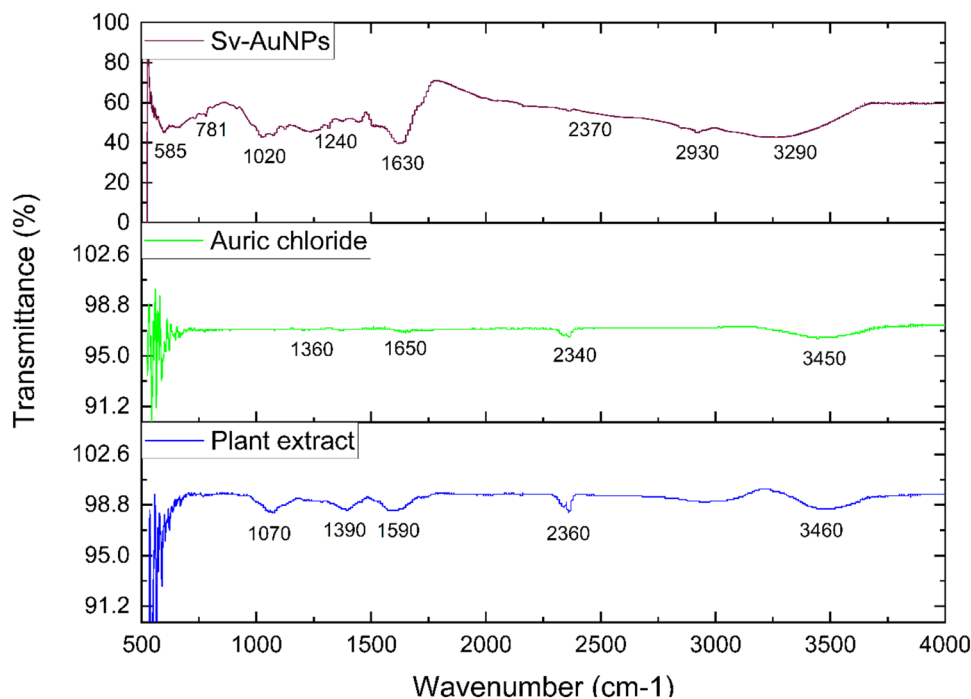


Fig. 4 Zeta potential (a) and size distribution (b) of Sv-AuNPs

Fig. 5 FTIR spectrum of plant extract, HAuCl<sub>4</sub> and Sv-AuNPs



% Inhibition of DPP Hradical

$$= \left\{ \frac{(\text{Abs}_{\text{control}} - \text{Abs}_{\text{sample}})}{\text{Abs}_{\text{control}}} \times 100 \right\} \quad (1)$$

Here,

Abs<sub>control</sub>- absorbance of DPPH; Abs<sub>sample</sub>- absorbance of Sv-AuNPs/ plant extract/ascorbic acid.

**Catalytic activity** The catalytic potential of Sv-AuNPs was analyzed against degradation of CR and 4-NP [32].

Freshly prepared solution of CR (1 mM)/ 4-NP (0.4 mM) and NaBH<sub>4</sub> (0.15 M) was diluted to make a volume of 3 ml and treated with 200 μl of Sv-AuNPs (50 μg/ml). Solution without Sv-AuNPs was used as the control.

**Statistical analysis** Graphical analysis was done using Microsoft Excel and Origin Pro-2021. Data is presented as mean value ± SE and p < 0.05 was taken as statistically significant.

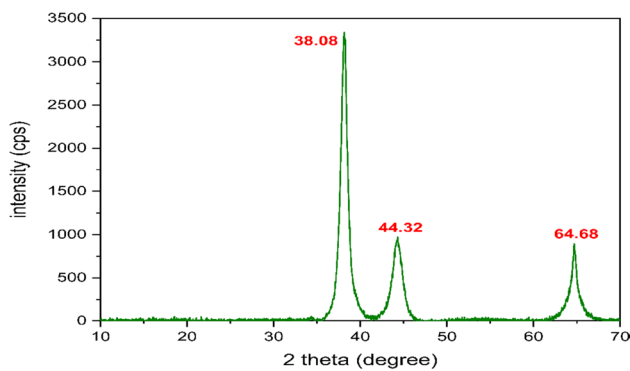
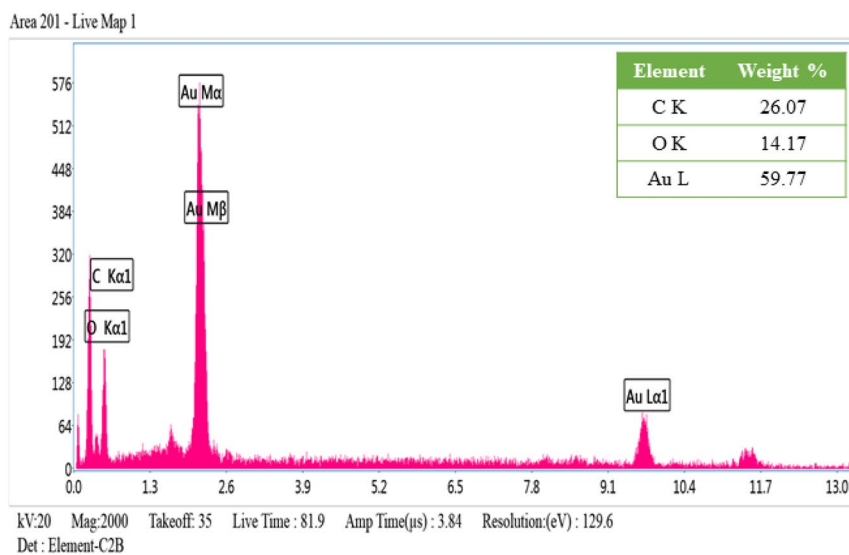


Fig. 6 XRD spectrum of Sv-AuNPs

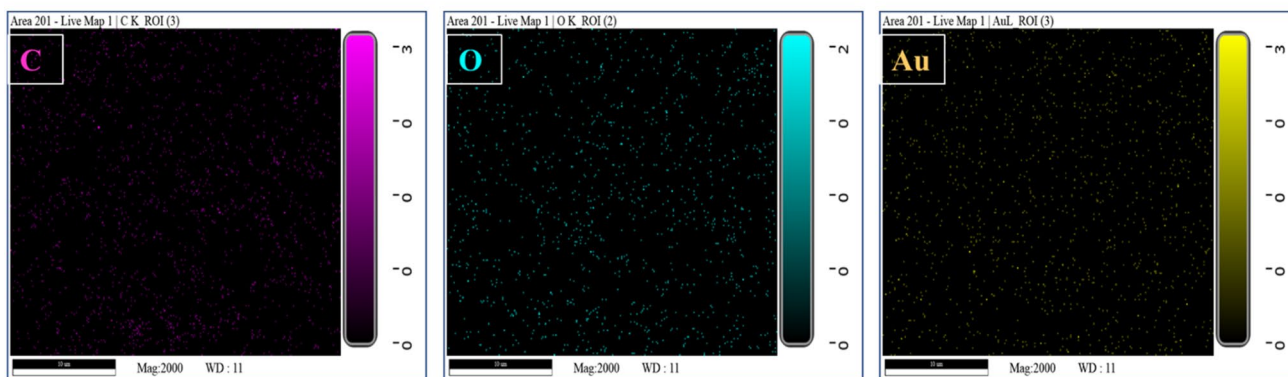
### Results and Discussion

*Plausible Mechanism for Synthesis of Nanoparticles* It is anticipated that biogenic synthesis involves two steps: firstly, phytoconstituents aid in the reduction of Au<sup>3+</sup> to Au<sup>0</sup> and then agglomeration and stabilization leads to the formation of nanoparticles. The probable mechanism for synthesis of Sv-AuNPs is depicted in Fig. 2.

*UV–Vis Spectrum* A strong peak at 536 nm confirmed the synthesis of Sv-AuNPs. Appearance of this peak could be attributed to the surface plasmon resonance (SPR) of AuNPs [33]. Our findings are in line with Mie theory, which states that small-sized nanoparticles exhibits a single peak in UV spectra [34]. Other researchers have also reported SPR phenomenon for AuNPs synthesis and their absorption in the range of 500 to 550 nm [35–37]. UV analysis was carried out upto 180 days and the peak position remained



(a)



(b)

Fig. 7 EDS spectrum (a) elemental mapping image of ‘C’, ‘O’, & ‘Au’ (b) of Sv-AuNPs

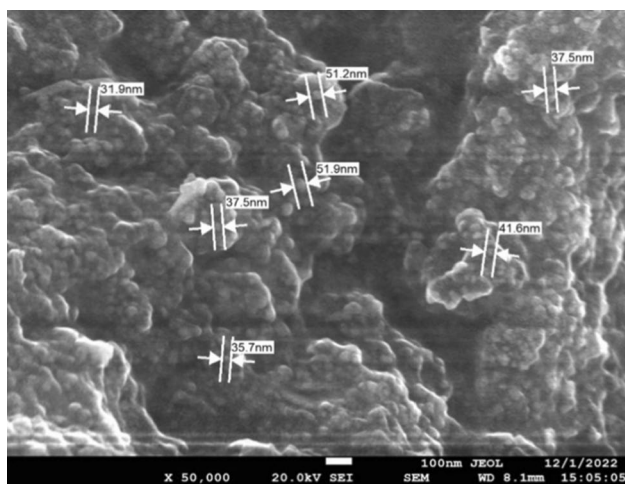


**Fig. 8** FE-SEM monograph of Sv-AuNPs

constant indicating that no aggregation occurred and size of Sv-AuNPs was stable upto six months (Fig. 3) [38, 39].

**Zeta Potential and DLS** Zeta potential was recorded to identify the surface charge of fabricated Sv-AuNPs and negative value of zeta potential indicated them to be wrapped with anions ( $-30.7$  mV). High electrostatic repulsive forces helps in stabilization of nanoparticles and prevents their aggregation [40, 41]. The particle size in liquid or suspension form was measured using DLS analysis and each and every particle was found to have a hydrodynamic diameter

of 160 nm (Fig. 4a, b). Low polydispersity index ( $PDI=0.2$ ) indicated Sv-AuNPs to have a narrow size distribution and monodisperse nature [28, 42].

**FTIR Spectrum** Characteristic peaks of alcohols, amines and aromatic compounds were observed from FTIR spectrum of Sv-AuNPs (Fig. 5). Here, strong and broad peak at  $3290\text{ cm}^{-1}$  and  $3460\text{ cm}^{-1}$  depicts O–H or N–H stretching of carbohydrates and proteins in the Sv-AuNPs and plant extract, respectively [43]. Other adsorption peaks at  $2930$  and  $2370\text{ cm}^{-1}$  are due to C–H stretching of alkanes and O=C=O stretching respectively [44]. Plant extract also showed a peak at  $2360\text{ cm}^{-1}$  which is attributed to stretching of O=C=O group. A strong peak at  $1630\text{ cm}^{-1}$  represents the C=N and C=C stretching of imine/oxime and alkene respectively. IR band at  $1240$  and  $1020\text{ cm}^{-1}$  shows O–H bending of phenols and S=O stretching and CO–O–CO stretching of sulfoxide and anhydride respectively. These peaks indicate that Sv-AuNPs are bound to proteins with the help of C=O group [45, 46]. Bands at  $781$  and  $595\text{ cm}^{-1}$  represents the aromatic C–H bending and C–Cl stretching of halo compounds respectively [28, 47, 48]. All these peaks indicated the presence of different functional groups that aid in the reduction of Au cations to AuNPs and help in capping and stabilization of Sv-AuNPs.

**XRD Analysis** Sharp peaks at  $2\theta$  of  $38.08$ ,  $44.32$ , and  $64.68$  degrees were recorded by XRD (Fig. 6). These are comparable to (111), (200), and (220) planes and Bragg reflections for face-centered cubic (fcc) and crystalline

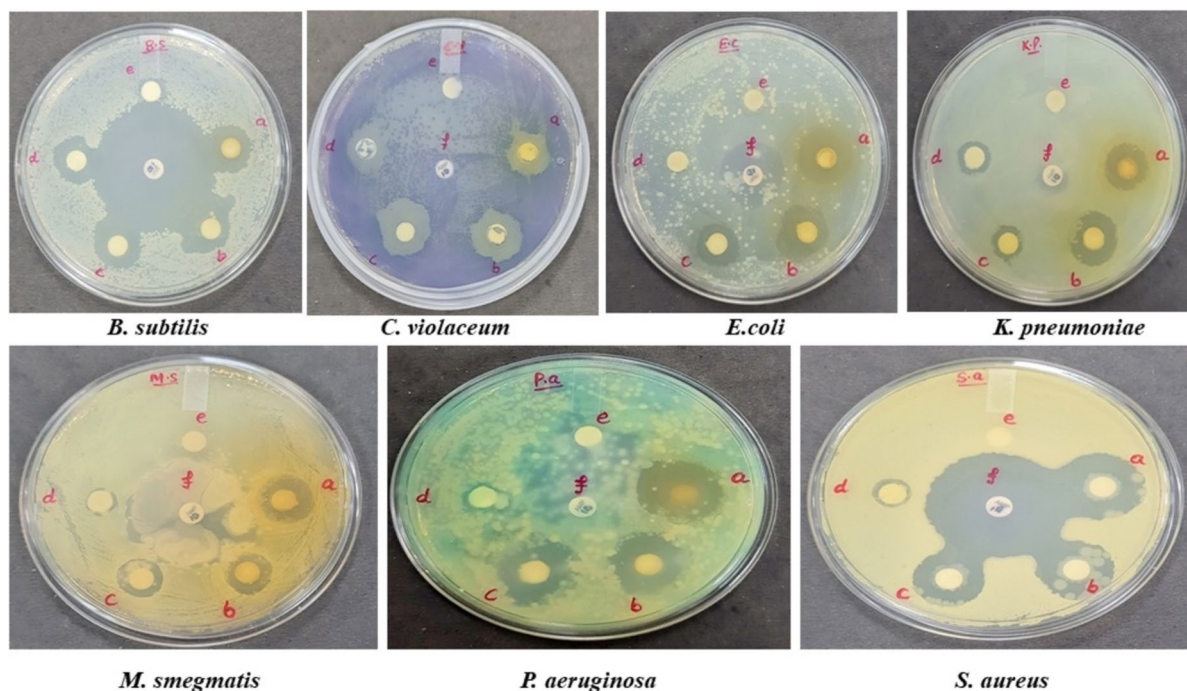


**Fig. 9** Disc diffusion assay: **a** Sv-AuNPs (5 mg/ml); **b** Sv-AuNPs (2 mg/ml); **c** Sv-AuNPs (1 mg/ml); **d** plant extract (100 mg/ml); **e** negative control; **f** ampicillin

**Fig. 10** ZOI obtained against tested bacterial strains

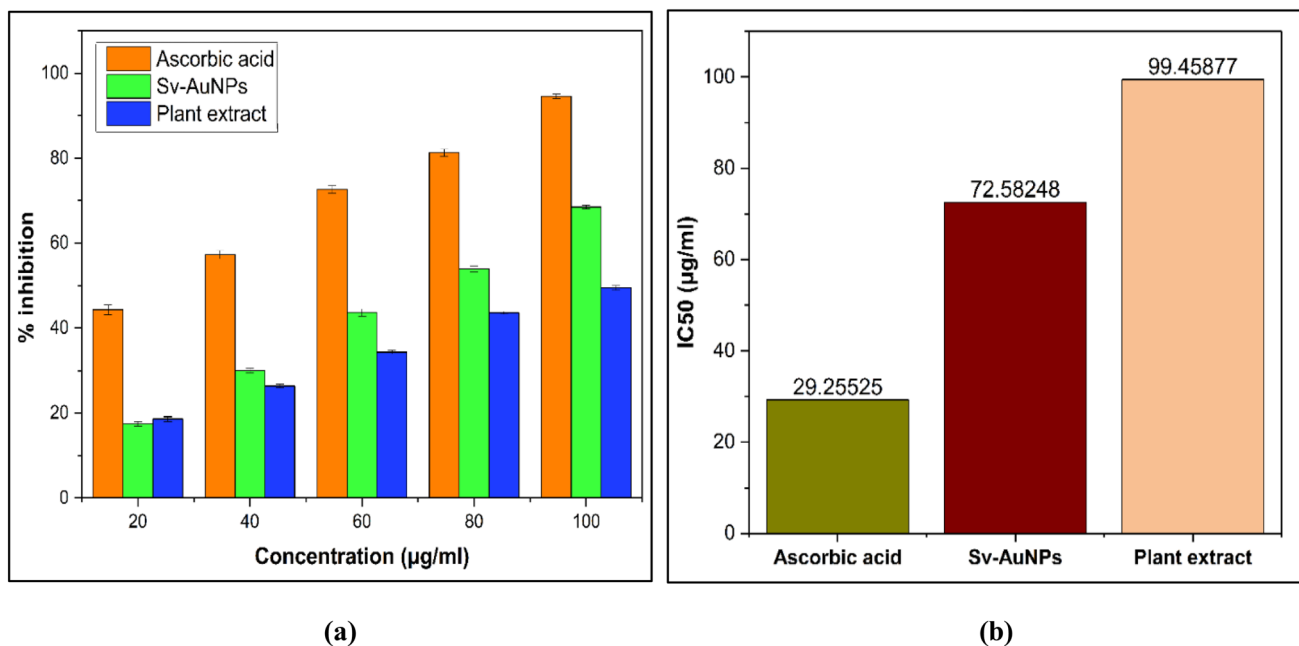
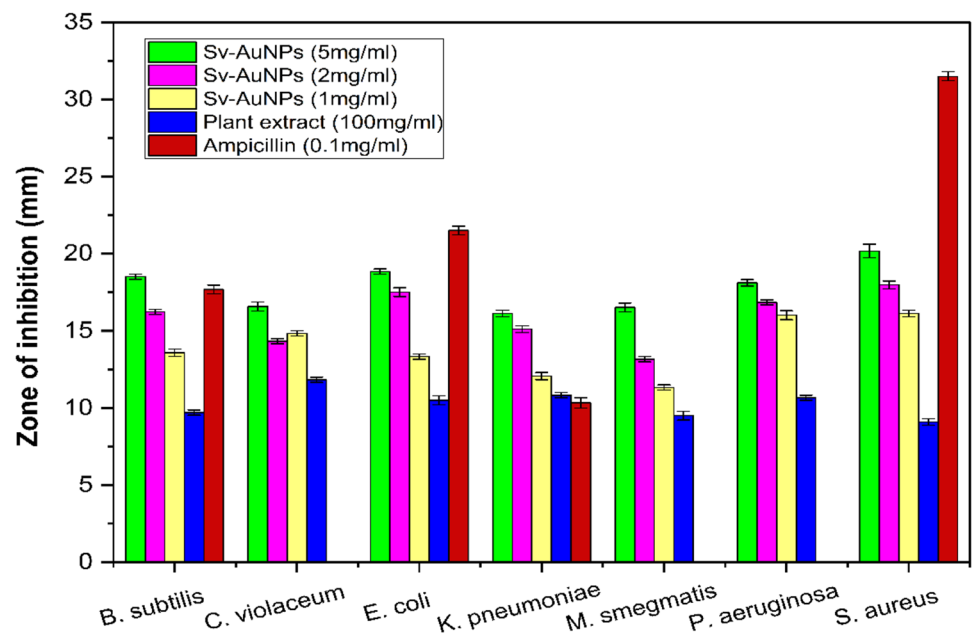


**Fig. 11** % inhibition (a) and IC<sub>50</sub> value (b) of ascorbic acid, Sv-AuNPs and plant extract

feature of Sv-AuNPs [28, 49, 50]. The absence of any additional peak in the spectrum signifies the purity of sample.

**EDS Analysis** A strong and clear peak at 2.2 keV in EDS spectrum confirmed the presence of gold in Sv-AuNPs (Fig. 7a). However, few signals of carbon and oxygen are also visible which might be attributable to various functional groups of plant extract. EDS mapping shows uniform distribution of carbon and oxygen along with gold metal ions and indicating that Sv-AuNPs are highly pure in nature (Fig. 7b).

Similar findings are also reported by other researchers [28, 51, 52].

**FE-SEM** FE-SEM images showed synthesized Sv-AuNPs to be spherical in shape and size ranging from 29-51 nm (Fig. 8).

**Antibacterial Studies** When Sv-AuNPs and aqueous plant extract were assessed for their antibacterial potential against different bacterial strains, aqueous plant extract showed lower ZOI as compared to Sv-AuNPs (Figs. 9, 10). Highest



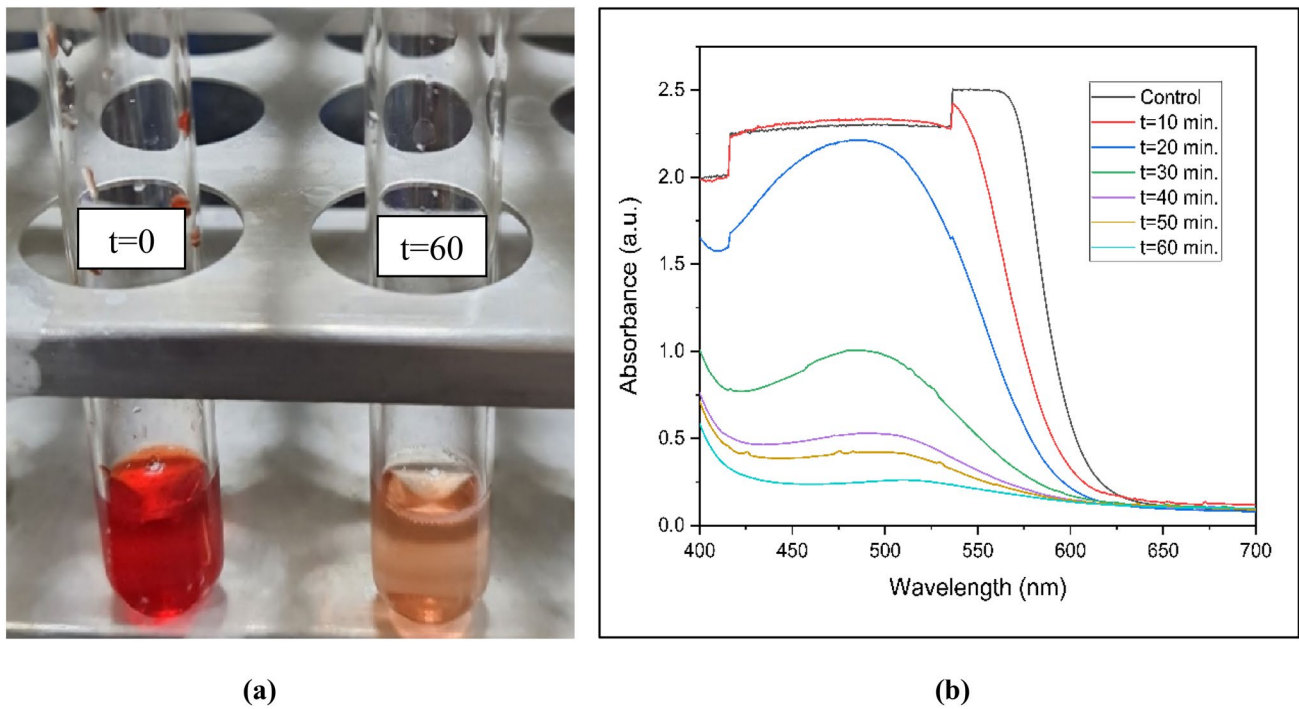


**Fig. 12** Reduction of CR in the presence of Sv-AuNPs: visual observation of color change (a) and UV–Vis spectrum at different time intervals (b)

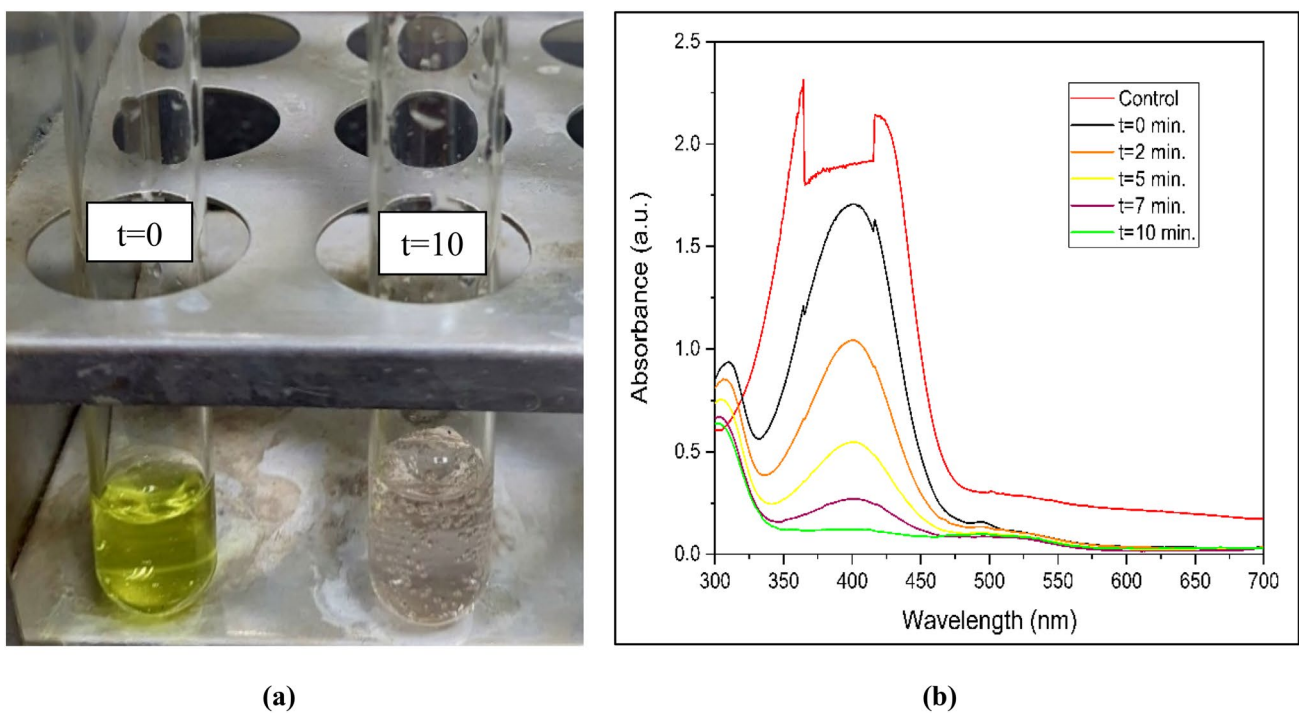


**Fig. 13** Reduction of 4-NP in the presence of Sv-AuNPs: visual observation of color change (a) and UV–Vis spectrum at different time intervals (b)

inhibitory activity of Sv-AuNPs was observed against *S. aureus* ( $20.1 \pm 0.4$  mm) followed by *E. coli*, *B. subtilis*, *P. aeruginosa*, *C. violaceum*, *M. smegmatis*. Amidst having the lowest antibacterial efficacy against *K. pneumoniae* ( $16.1 \pm 0.20$  mm), Sv-AuNPs outperformed the positive control ( $10.3 \pm 0.33$  mm). In case of *P. aeruginosa*, *C. violaceum* and *M. smegmatis* no ZOI was detected with standard antibiotic. However, Sv-AuNPs exhibited a remarkable ZOI against *P. aeruginosa* ( $18.1 \pm 0.20$  mm), *C. violaceum* ( $16.5 \pm 0.29$  mm), and *M. smegmatis* ( $16.5 \pm 0.28$  mm). This clearly demonstrated the role of Sv-AuNPs as a potent substitute to antibiotics and in combating bacterial infections. High antibacterial potential of Sv-AuNPs is possibly due to nanoparticles' small size and large surface area, which allows them to easily pierce bacterial cell wall, causing DNA and mitochondrial damage leading to cell death [50, 53–55]. Furthermore, it could be attributed to the synergistic effect of Sv-AuNPs capped with phytochemicals which are known to possess biological properties [56]. This is the first report on antibacterial activity of Sv-AuNPs. However researchers from different regions have reported significant antibacterial properties of gold, nickel, zinc, and silver nanoparticles synthesized from various other *Solanum* species [57–59].

**Antioxidant studies** For evaluating the antioxidant potential of plant extract, Sv-AuNPs and ascorbic acid; five different concentrations (20–100 µg/ml) of each were prepared from a stock solution of 1 mg/ml. A direct relationship between the concentration and percentage inhibition of Sv-AuNPs was observed in DPPH assay. % inhibition varied from  $17.44 \pm 0.53\%$  to  $68.47 \pm 0.42\%$  and  $18.60 \pm 0.55\%$  to  $49.41 \pm 0.53\%$  for Sv-AuNPs and aqueous plant extract, respectively (Fig. 11a).  $IC_{50}$  values obtained for Sv-AuNPs (72.58 µg/ml), plant extract (99.45 µg/ml), and ascorbic acid (29.25 µg/ml) are shown in Fig. 11b. Sv-AuNPs were found to possess higher antioxidant potential than plant extract. Because of the smaller size and large surface area of AuNPs, DPPH radicals are easily adsorbed onto the surface and trap H-atoms from AuNPs to form DPPH-H molecules, which accounts for their significantly high antioxidant activity [60]. Besides, different phytochemicals binds to the surface of the nanoparticles during the synthesis process and enhance antioxidant activity of nanoparticles [61]. Our findings are comparable to those reported by other research groups [62, 63].

**Catalytic activity** Catalytic efficacy of Sv-NPs (50 µg/ml) was analyzed against degradation of CR and 4-NP at room temperature. Time dependent degradation of the dye was observed visually by color change from red/pale yellow to colorless and by analyzing the UV–Vis spectrum in range of 300–700 nm (Figs. 12, 13). In accordance with the UV–Vis spectrum of CR, the initial absorption maxima recorded was at 570 nm, decreased gradually after the addition of Sv-NPs

and it disappeared within one hour. 4-NP, on the other hand, showed a bright yellow color with a strong peak at 430 nm. The probable mechanism that aids in the reduction of 4-NP is that on addition of Sv-AuNPs, sodium phenolate is reduced to 4-aminophenol making the solution colorless and shift in peak from 430 to 300 nm.  $NaBH_4$  alone was not found to have any catalytic activity against harmful dyes and degradation occurs only after addition of Sv-AuNPs [32, 64]. Similar findings were also reported with nanoparticles synthesized from plants belonging to Arecaceae, Salicaceae, Solanaceae, and Zingiberaceae families from other parts of the world [65–68].

## Conclusion

In present study, one-pot, simple and cost-effective approach for synthesis of Sv-AuNPs from *S. virginianum* was used. Phytochemicals present in aqueous plant extract served as reducing and stabilizing agents, enabling synthesis of Sv-AuNPs within 15–20 min. Microscopic and spectroscopic techniques were used to characterize Sv-AuNPs. UV–Vis spectrum showed them to be stable at room temperature for up to six months. Sv-AuNPs obtained were monodispersed, spherical in shape, and ~33 nm in size. They exhibited higher antibacterial and antioxidant potential as compared to the aqueous plant extract. Interestingly, Sv-AuNPs showed ZOI even higher than standard antibiotic against some of the tested bacterial strains. These properties make them an indispensable agent to fight against diseases of the diverse origin. Sv-AuNPs also aid in environmental remediation by rapidly degrading harmful dyes like CR and 4-NP. The above findings revealed that Sv-AuNPs can function as an antibacterial agent, DPPH radical scavenger and catalysts. The plant appears to be a promising candidate in nanotherapeutics and environmental remediation being a repository of bioactive compounds. However, more research work is required to validate the role of biosynthesized nanoparticles in clinical and ecological fields.

**Acknowledgements** We are thankful to the Department of Botany and Aryabhata Central Instrumentation Laboratory (ACIL), Maharshi Dayanand University, Rohtak for providing necessary facilities and support to carry out this study.

**Author contribution** Conceptualization: PR; Methodology: PR; Writing—original draft preparation: PR; Writing—review and editing: PR, AC; Supervision: PD.

**Funding** No funding was received for conducting this study.

**Availability of data and material** Not Applicable.

## Declarations

**Conflict of interest** The authors have no relevant financial or non-financial interests to disclose.

**Ethics approval and consent to participate** Not Applicable.

**Consent for publication** Not Applicable.

**Availability of data and material** Not Applicable.

## References

- Beyene HD, Werkneh AA, Bezabh HK, Ambaye TG (2017) Synthesis paradigm and applications of silver nanoparticles (AgNPs), a review. *Sustain Mater Technol* 13:18–23. <https://doi.org/10.1016/J.SUSMAT.2017.08.001>
- Baig N, Kammakam I, Falath W, Kammakam I (2021) Nanomaterials: a review of synthesis methods, properties, recent progress, and challenges. *Mater Adv* 2:1821–1871. <https://doi.org/10.1039/D0MA00807A>
- Chaloupka K, Malam Y, Seifalian AM (2010) Nanosilver as a new generation of nanoparticle in biomedical applications. *Trends Biotechnol* 28:580–588. <https://doi.org/10.1016/J.TIBTECH.2010.07.006>
- Muddineti OS, Ghosh B, Biswas S (2015) Current trends in using polymer coated gold nanoparticles for cancer therapy. *Int J Pharm* 484:252–267. <https://doi.org/10.1016/J.IJPHARM.2015.02.038>
- Sztandera K, Gorzkiewicz M, Klajnert-Maculewicz B (2019) Gold nanoparticles in cancer treatment. *Mol Pharm* 16:1–23. [https://doi.org/10.1021/ACS.MOLPHARMACEUT.8B00810/ASSET/IMAGES/MEDIUM/MP-2018-00810X\\_0015.GIF](https://doi.org/10.1021/ACS.MOLPHARMACEUT.8B00810/ASSET/IMAGES/MEDIUM/MP-2018-00810X_0015.GIF)
- Nejati K, Dadashpour M, Gharibi T et al (2022) Biomedical applications of functionalized gold nanoparticles: a review. *J Clust Sci* 33:1–16. <https://doi.org/10.1007/S10876-020-01955-9/FIGURES/4>
- Huang X, El-Sayed MA (2010) Gold nanoparticles: optical properties and implementations in cancer diagnosis and photothermal therapy. *J Adv Res* 1:13–28. <https://doi.org/10.1016/J.JARE.2010.02.002>
- Zhang, (2015) Gold nanoparticles: recent advances in the biomedical applications. *Cell Biochem Biophys* 72:771–775. <https://doi.org/10.1007/S12013-015-0529-4/FIGURES/2>
- Elashmawi IS, Elsayed NH (2020) The role of gold nanoparticles in the structural and electrical properties of Cs/PVP blend. *Polym Bull* 77:949–962. <https://doi.org/10.1007/S00289-019-02786-Z/FIGURES/7>
- Jia YP, Ma BY, Wei XW, Qian ZY (2017) The in vitro and in vivo toxicity of gold nanoparticles. *Chinese Chem Lett* 28:691–702. <https://doi.org/10.1016/J.CCLET.2017.01.021>
- Cabuzu D, Cirja A, RP-C topics in, 2015 U (2015) Biomedical applications of gold nanoparticles. *Curr Top Med Chem* 15:1605–1613
- Aminabad NS, Farshbaf M, Akbarzadeh A (2019) Recent advances of gold nanoparticles in biomedical applications: state of the art. *Cell Biochem Biophys* 77:123–137. <https://doi.org/10.1007/S12013-018-0863-4/FIGURES/14>
- Mikhailova EO (2021) Gold nanoparticles: biosynthesis and potential of biomedical application. *J Funct Biomater*. 12:70. <https://doi.org/10.3390/JFB12040070>
- Patel SKS, Otari SV, Li J et al (2018) Synthesis of cross-linked protein-metal hybrid nanoflowers and its application in repeated batch decolorization of synthetic dyes. *J Hazard Mater* 347:442–450
- Zan G, Wu Q (2016) Biomimetic and bioinspired synthesis of nanomaterials/nanostructures. *Adv Mater* 28:2099–2147. <https://doi.org/10.1002/ADMA.201503215>
- Ansary AA, Syed A, Elgorban AM et al (2022) Neodymium selenide nanoparticles: greener synthesis and structural characterization. *Biomimetics* 7:150. <https://doi.org/10.3390/BIOMIMETICS7040150>
- Nath D, Banerjee P (2013) Green nanotechnology: a new hope for medical biology. *Environ Toxicol Pharmacol* 36:997–1014. <https://doi.org/10.1016/J.ETAP.2013.09.002>
- Otari SV, Patel SKS, Kalia VC et al (2019) Antimicrobial activity of biosynthesized silver nanoparticles decorated silica nanoparticles. *Indian J Microbiol* 59:379–382
- Govindaraju K, Kiruthiga V, Manikandan R et al (2011)  $\beta$ -Glucosidase assisted biosynthesis of gold nanoparticles: a green chemistry approach. *Mater Lett* 65:256–259. <https://doi.org/10.1016/J.MATLET.2010.09.078>
- Elbagory AM, Cupido CN, Meyer M, Hussein AA (2016) Large scale screening of Southern African plant extracts for the green synthesis of gold nanoparticles using microtitre-plate method. *Mol* 21:1498. <https://doi.org/10.3390/MOLECULES21111498>
- Hassanisaadi M, Bonjar GHS, Rahdar A et al (2021) Environmentally safe biosynthesis of gold nanoparticles using plant water extracts. *Nanomater* 11:2033. <https://doi.org/10.3390/NANO11082033>
- Parmar S, Gangwal A, Navin S (2010) *Solanum xanthocarpum* (Yellow Berried Night Shade): a review a review on natural fiber and its hybrid composite plastic materials view project detail study on *Bombax ceiba* prickly view project. *Der Pharm Lett* 2:373–383
- Parmar KM, Itankar PR, Joshi A, Prasad SK (2017) Anti-psoriatic potential of *Solanum xanthocarpum* stem in Imiquimod-induced psoriatic mice model. *J Ethnopharmacol* 198:158–166. <https://doi.org/10.1016/J.JEP.2016.12.046>
- Borgato L, Pisani F, Furini A (2007) Plant regeneration from leaf protoplasts of *Solanum virginianum* L. (*Solanaceae*). *Plant Cell Tissue Organ Cult* 88:247–252. <https://doi.org/10.1007/S11240-006-9196-X/FIGURES/1>
- Govindan S, Viswanathan S, Vijayasekaran V, Alagappan R (1999) A pilot study on the clinical efficacy of *Solanum xanthocarpum* and *Solanum trilobatum* in bronchial asthma. *J Ethnopharmacol* 66:205–210. [https://doi.org/10.1016/S0378-8741\(98\)00160-3](https://doi.org/10.1016/S0378-8741(98)00160-3)
- Kumar S, Pandey AK (2014) Medicinal attributes of *Solanum xanthocarpum* fruit consumed by several tribal communities as food: an in vitro antioxidant, anticancer and anti HIV perspective. *BMC Complement Altern Med* 14:1–8. <https://doi.org/10.1186/1472-6882-14-112/FIGURES/4>
- Javaid U, Javaid S, Ashraf W et al (2021) Chemical profiling and dose-dependent assessment of fear reducing and memory-enhancing effects of *Solanum virginianum* in rats. *Dose Response* 19:1–18. <https://doi.org/10.1177/1559325821998486>
- Zhang P, Wang P, Yan L, Liu L (2018) Synthesis of gold nanoparticles with *Solanum xanthocarpum* extract and their in vitro anticancer potential on nasopharyngeal carcinoma cells. *Int J Nanomed* 13:7047
- Aljabali AAA, Akkam Y, Al Zoubi MS et al (2018) Synthesis of gold nanoparticles using leaf extract of *ziziphus zizyphus* and their antimicrobial activity. *Nanomater* 8:174. <https://doi.org/10.3390/NANO8030174>
- Bauer AW, Kirby WM, Sherris JC, Turck M (1966) Antibiotic susceptibility testing by a standardized single disk method. *Am J*

- Clin Pathol 45:493–496. [https://doi.org/10.1093/AJCP/45.4\\_TS.493](https://doi.org/10.1093/AJCP/45.4_TS.493)
31. Mensor LL, Menezes FS, Leitão GG et al (2001) Screening of Brazilian plant extracts for antioxidant activity by the use of DPPH free radical method. *Phyther Res* 15:127–130
  32. Mata R, Bhaskaran A, Sadras SR (2016) Green-synthesized gold nanoparticles from *Plumeria alba* flower extract to augment catalytic degradation of organic dyes and inhibit bacterial growth. *Particuology* 24:78–86. <https://doi.org/10.1016/J.PARTIC.2014.12.014>
  33. Elia P, Zach R, Hazan S et al (2014) Green synthesis of gold nanoparticles using plant extracts as reducing agents. *Int J Nanomed* 9:4007. <https://doi.org/10.2147/IJN.S57343>
  34. Pechyen C, Ponsanti K, Tangnorawich B, Ngernyuang N (2021) Waste fruit peel – Mediated green synthesis of biocompatible gold nanoparticles. *J Mater Res Technol* 14:2982–2991. <https://doi.org/10.1016/j.jmrt.2021.08.111>
  35. Narayanan KB, Sakthivel N (2010) Phytosynthesis of gold nanoparticles using leaf extract of *Coleus amboinicus* Lour. *Mater Charact* 61:1232–1238. <https://doi.org/10.1016/J.MATCHAR.2010.08.003>
  36. Rhim JW, Kanmani P (2015) Synthesis and characterization of biopolymer agar mediated gold nanoparticles. *Mater Lett* 141:114–117. <https://doi.org/10.1016/J.MATLET.2014.11.069>
  37. Soto KM, López-Romero JM, Mendoza S et al (2023) Rapid and facile synthesis of gold nanoparticles with two Mexican medicinal plants and a comparison with traditional chemical synthesis. *Mater Chem Phys* 295:127109. <https://doi.org/10.1016/J.MATCHEMPHYS.2022.127109>
  38. Haiss W, Thanh NTK, Aveyard J, Fernig DG (2007) Determination of size and concentration of gold nanoparticles from UV-Vis spectra. *Anal Chem* 79:4215–4221. [https://doi.org/10.1021/AC0702084/SUPPL\\_FILE/AC0702084SI20070321\\_014144.PDF](https://doi.org/10.1021/AC0702084/SUPPL_FILE/AC0702084SI20070321_014144.PDF)
  39. Oliveira JP, Prado AR, Keijkow WJ et al (2020) A helpful method for controlled synthesis of monodisperse gold nanoparticles through response surface modeling. *Arab J Chem* 13:216–226. <https://doi.org/10.1016/J.ARABJC.2017.04.003>
  40. Dash SS, Bag BG, Hota P (2015) *Lantana camara* Linn leaf extract mediated green synthesis of gold nanoparticles and study of its catalytic activity. *Appl Nanosci* 5:343–350. <https://doi.org/10.1007/S13204-014-0323-4/FIGURES/6>
  41. Al-Radadi NS (2021) Facile one-step green synthesis of gold nanoparticles (AuNp) using licorice root extract: antimicrobial and anticancer study against HepG2 cell line. *Arab J Chem* 14:102956. <https://doi.org/10.1016/J.ARABJC.2020.102956>
  42. Hussain MH, Abu Bakar NF, Low KF et al (2021) Growth-controlled synthesis of polymer-coated colloidal-gold nanoparticles using electrospray-based chemical reduction. *Particuology* 57:72–81. <https://doi.org/10.1016/J.PARTIC.2020.12.004>
  43. Zhang L, He Y, Feng S et al (2016) Preparation and tribological properties of novel boehmite/graphene oxide nano-hybrid. *Ceram Int* 42:6178–6186. <https://doi.org/10.1016/J.CERAMINT.2015.12.178>
  44. Kočišová E, Antalík A, Procházka M (2013) Drop coating deposition Raman spectroscopy of liposomes: role of cholesterol. *Chem Phys Lipids* 172–173:1–5. <https://doi.org/10.1016/J.CHEMPHYS-LIP.2013.04.002>
  45. Philip D (2010) Green synthesis of gold and silver nanoparticles using *Hibiscus rosa sinensis*. *Phys E Low-dimens Syst Nanostruct* 42:1417–1424. <https://doi.org/10.1016/J.PHYSE.2009.11.081>
  46. Aswathy AS, Philip D (2012) Green synthesis of gold nanoparticles using *Trigonella foenum-graecum* and its size-dependent catalytic activity. *Spectrochim Acta Part A Mol Biomol Spectrosc* 97:1–5. <https://doi.org/10.1016/J.SAA.2012.05.083>
  47. Kumar B, Smita K, Cumbal L et al (2016) One pot phytosynthesis of gold nanoparticles using *Genipa americana* fruit extract and its biological applications. *Mater Sci Eng C* 62:725–731. <https://doi.org/10.1016/J.MSEC.2016.02.029>
  48. Muniyappan N, Pandeewaran M, Amalraj A (2021) Green synthesis of gold nanoparticles using *Curcuma pseudomontana* isolated curcumin: Its characterization, antimicrobial, antioxidant and anti-inflammatory activities. *Environ Chem Ecotoxicol* 3:117–124. <https://doi.org/10.1016/J.ENCECO.2021.01.002>
  49. Das RK, Gogoi N, Bora U (2011) Green synthesis of gold nanoparticles using *Nyctanthes arbortristis* flower extract. *Bioprocess Biosyst Eng* 34:615–619. <https://doi.org/10.1007/S00449-010-0510-Y/FIGURES/5>
  50. Suriyakala G, Sathiyaraj S, Babujanathanam R et al (2022) Green synthesis of gold nanoparticles using *Jatropha integerrima* Jacq flower extract and their antibacterial activity. *J King Saud Univ Sci* 34:101830. <https://doi.org/10.1016/J.JKSUS.2022.101830>
  51. Suman TY, Radhika Rajasree SR, Ramkumar R et al (2014) The Green synthesis of gold nanoparticles using an aqueous root extract of *Morinda citrifolia* L. *Spectrochim Acta Part A Mol Biomol Spectrosc* 118:11–16. <https://doi.org/10.1016/J.SAA.2013.08.066>
  52. Patel SKS, Gupta RK, Kim S-Y et al (2021) Rhus vernicifera lacase immobilization on magnetic nanoparticles to improve stability and its potential application in bisphenol a degradation. *Indian J Microbiol* 61:45–54
  53. Panda SK, Mohanta YK, Padhi L et al (2016) Large scale screening of ethnomedicinal plants for identification of potential antibacterial compounds. *Molecules* 21:293. <https://doi.org/10.3390/MOLECULES21030293>
  54. Varghese BA, Nair RVR, Jude S et al (2021) Green synthesis of gold nanoparticles using *Kaempferia parviflora* rhizome extract and their characterization and application as an antimicrobial, antioxidant and catalytic degradation agent. *J Taiwan Inst Chem Eng* 126:166–172. <https://doi.org/10.1016/j.jtice.2021.07.016>
  55. Otari SV, Patel SKS, Kim S-Y et al (2019) Copper ferrite magnetic nanoparticles for the immobilization of enzyme. *Indian J Microbiol* 59:105–108
  56. Chithambharan A, Pottail L, Mirlle RM et al (2021) Bioinspired gold nanoparticle synthesis using *Terminalia bellerica* fruit parts and exploring their anti-bacterial potency in vitro. *Indian J Microbiol* 61:298–305
  57. Sengottaiyan A, Mythili R, Selvankumar T et al (2016) Green synthesis of silver nanoparticles using *Solanum indicum* L. and their antibacterial, splenocyte cytotoxic potentials. *Res Chem Intermed* 42:3095–3103. <https://doi.org/10.1007/s11164-015-2199-7>
  58. Ezhilarasi AA, Vijaya JJ, Kaviyarasu K et al (2020) Green synthesis of nickel oxide nanoparticles using *Solanum trilobatum* extract for cytotoxicity, antibacterial and photocatalytic studies. *Surfaces Interfaces* 20:100553. <https://doi.org/10.1016/j.surfin.2020.100553>
  59. Muthuvel A, Adavallan K, Balamurugan K, Krishnakumar N (2014) Biosynthesis of gold nanoparticles using *Solanum nigrum* leaf extract and screening their free radical scavenging and antibacterial properties. *Biomed Prev Nutr* 4:325–332. <https://doi.org/10.1016/j.bionut.2014.03.004>
  60. Fouda MMG, Ajarem JS, Maodaa SN et al (2020) Carboxymethyl cellulose supported green synthetic features of gold nanoparticles: antioxidant, cell viability, and antibacterial effectiveness. *Synth Met* 269:116553. <https://doi.org/10.1016/J.SYNTHMET.2020.116553>
  61. Rajan A, Vilas V, Philip D (2015) Studies on catalytic, antioxidant, antibacterial and anticancer activities of biogenic gold nanoparticles. *J Mol Liq* 212:331–339
  62. Singh L, Antil R, Dahiya P (2021) Antimicrobial and antioxidant potential of vernonia cinerea extract coated AuNPs. *Indian J Microbiol* 61:506–518. <https://doi.org/10.1007/S12088-021-00976-W/FIGURES/9>

63. Sathishkumar G, Jha PK, Vignesh V et al (2016) Cannonball fruit (*Couroupita guianensis*, Aubl.) extract mediated synthesis of gold nanoparticles and evaluation of its antioxidant activity. *J Mol Liq* 215:229–236. <https://doi.org/10.1016/J.MOLLIQ.2015.12.043>
64. Umamaheswari C, Lakshmanan A, Nagarajan NS (2018) Green synthesis, characterization and catalytic degradation studies of gold nanoparticles against congo red and methyl orange. *J Photochem Photobiol B Biol* 178:33–39. <https://doi.org/10.1016/J.JPHOTOBIOL.2017.10.017>
65. Zayed MF, Eisa WH (2014) *Phoenix dactylifera* L. leaf extract phytosynthesized gold nanoparticles; controlled synthesis and catalytic activity. *Spectrochim Acta Part A Mol Biomol Spectrosc* 121:238–244. <https://doi.org/10.1016/J.SAA.2013.10.092>
66. Nadaf NY, Kanase SS (2019) Biosynthesis of gold nanoparticles by *Bacillus marisflavi* and its potential in catalytic dye degradation. *Arab J Chem* 12:4806–4814. <https://doi.org/10.1016/J.ARA-BJC.2016.09.020>
67. Guliani A, Kumari A, Acharya A (2021) Green synthesis of gold nanoparticles using aqueous leaf extract of *Populus alba*: characterization, antibacterial and dye degradation activity. *Int J Environ Sci Technol* 18:4007–4018. <https://doi.org/10.1007/S13762-020-03065-5/FIGURES/4>
68. Patil TP, Vibhute AA, Patil SL et al (2023) Green synthesis of gold nanoparticles via *Capsicum annum* fruit extract: characterization, antiangiogenic, antioxidant and anti-inflammatory activities. *Appl Surf Sci Adv* 13:100372. <https://doi.org/10.1016/j.apsadv.2023.100372>

**Publisher's Note** Springer Nature remains neutral with regard to jurisdictional claims in published maps and institutional affiliations.

Springer Nature or its licensor (e.g. a society or other partner) holds exclusive rights to this article under a publishing agreement with the author(s) or other rightsholder(s); author self-archiving of the accepted manuscript version of this article is solely governed by the terms of such publishing agreement and applicable law.